DOI https: //doi. org/10.1007/s11595-019-2029-7

Microstructures and Tensile Properties of Hot-extruded Mg-6Zn-*x*Ce (*x*=0, 0.6, 1.0, 2.0) Alloys

YU Heshuai [1], YANG Wenpeng[1,2*], CUI Hongbao[1,2], GUO Xuefeng[1,2], WANG Ying[1], WU Yali[1]

(1. School of Materials Science and Engineering, Henan Polytechnic University, Jiaozuo 454000, China; 2.Henan International Joint Research Laboratory for High-Performance Light Metallic Materials and Numerical Simulations, Henan Polytechnic University, Jiaozuo 454000, China)

Abstract: Mg-6Zn-*x*Ce (*x* = 0, 0.6, 1.0, 2.0) alloy ingots with diameter of 50 mm were extruded into bars with diameter of 12 mm at 300 ℃. The microstructures were analyzed by X-ray diffraction, optical microscopy, scanning electron microscopy and transmission electron microscopy, and mechanical properties were tested at room temperature. The results showed that major intermetallic composition in as-cast Mg-6Zn and Mg-6Zn-0.6Ce alloys was Mg_4Zn_7 phase, during extrusion Mg_4Zn_7 phase was dissolved into matrix and then precipitated as $MgZn_2$. In as-cast and as-extruded Mg-6Zn-1Ce and Mg-6Zn-2Ce alloys the major intermetallic composition was T phase. The microstructure of as-extruded alloy was refined due to complete dynamic recrystallization, the average grain size decreased with increasing Ce content, which were 12.1, 11.7, 11.0 and 10.0 μm, respectively. High density $MgZn_2$ precipitated in Mg-6Zn and Mg-6Zn-0.6Ce alloys. The broken T phase particles were distributed linearly along extrusion direction. Mg-6Zn-0.6Ce alloy exhibited a high yield strength of 226.3 MPa that was about 24 MPa higher than Mg-6Zn alloy. However, with increasing Ce contents, the strengths were decreased slightly because the effects of precipitation strengthening of $MgZn_2$ and solid solute strengthening of Zn were weakened though the strengthening effect of T phase was enhanced.

Key words: magnesium alloy; extrusion; microstructure; mechanical properties

1 Introduction

Magnesium alloys have been received much attention for the application in automobile, aerospace, light rail, high speed trains and electronic industry owing to their low density, high specific strength, good castability and excellent damping property[1]. However, their applications are very limited because magnesium alloys have low strength and limited ductility at ambient temperature resulted from their hexagonal close-packed structure. Mg-Zn alloy system, which has high strength and significant aging strengthening effect[2,3], is one of the alloys that have the most consumable quantities in engineering application. The disadvantage of low eutectic temperature of Mg-Zn system alloys (about 340 ℃[4]) limits the application at elevated temperature. Fortunately, their strength and creep resistant at elevated temperatures can be improved by introducing rare-earth (RE) elements to form stable compounds[5,6]. As an important RE element, Ce has limited solid solubility in Mg[4]. With a trace addition of Ce less than 0.5 wt%, the basal plane texture of Mg alloy is modified effectively that leads to the stretch formability be improved significantly[7,8]. With the addition of Ce more than 1 wt%, the mechanical properties at elevated temperatures are enhanced resulting from the formation of stable strengthening phases, such as $Mg_{12}Ce$ and $Mg_{17}Ce_2$[9,10]. Previous reports of Mg-Zn-Ce alloys stress on the effects of Zn and Ce on modification of deformation texture. The additions of Zn and Ce in the studied alloys are no more than 2.5% and 0.2%, respectively, which mainly dissolved in Mg matrix[11,12]. In order to prepare Mg alloys with high performance, the comprehensive effect of the particle strengthening, precipitation strengthening and solution strengthening needs to be considered. Therefore, the additions of alloying elements should not be too little. In this paper, the effects of Ce on microstructure and mechanical properties in hot extruded Mg-6Zn alloy

(Received: Mar. 7, 2017; Accepted: Nov. 11, 2018)

YU Heshuai(于合帅): Ph D Candidate; E-mail:15978737565@163.com

*Corresponding author: YANG Wenpeng(杨文朋): Ph D; E-mail: wenpengy@hpu.edu.cn

Funded by the National Natural Science Foundation of China (No.51571086), China Postdoctoral Science Foundation (No. 2013M541973), The Research Fund for Doctoral Program of Henan Polytechnic University (No. B2015-14)

are studied; the evolution of phase constitution and the strengthening mechanism are discussed.

2 Experimental

2.1 Materials preparation

Mg-6Zn-*x*Ce (wt%, *x*=0, 0.6, 1.0, 2.0) alloys were prepared by melting Mg (>99.9% purity), Zn (>99.9% purity) and Mg-90%Ce master alloy in an electric resistance furnace at 720 ℃ under Ar + SF_6 atmosphere. The ingots with diameter of 52 mm were obtained by pouring melt into graphitic mould. Then the ingots were machined to rods with 50 mm in diameter and 60 mm in length for extrusion.

For the purpose of homogenizing the temperature of the billets, the billets and extrusion die were heated to 300 ℃ and hold for 60 min before extrusion. The extrusion was carried out under a pressure of 6.28×10^5 N and a speed of 10 mm/min. During extrusion process, the fluctuation of temperature is about ±3 ℃. Finally, the billets were extruded into bars with a diameter of 12 mm at an extrusion ratio of 17:1.

2.2 Microstructural analysis

The phase constitutions were analyzed by a RigakuD/max-3C X-ray (XRD) instrument with Cu Kα radiation, the scan angle ranges from 15° to 90° with a scanning step size of 0.033°. To observe the microstructure by optical microscopy, standard metallographic sample preparation techniques were employed, including grinding, polishing and the use of an etchant based upon picric acid which revealed the grain boundaries. The specimen cut parallel to extrusion direction (ED) was examined using a Niko Epiphot optical microscopy (OM). The average grain size was estimated from several micrographs using a computer aided linear intercept measurement. The morphology and distribution of broken strengthening particles were observed using a JSM-6700F scanning electron microscopy (SEM). Transmission electron microscopy (TEM) was employed to obtain detailed information about microstructure, such as precipitates and dislocations. Thin foils for the TEM observation were prepared from as-extruded materials by electropolishing in a solution of 15% HNO_3+85% CH_3OH at about −30 ℃. Finally, an ion miller was employed to remove the oxide film at an ion accelerating voltage of 4.0 kV. TEM observations were carried out using a JEM-3010 microscopy operating at 300 kV.

2.3 Mechanical properties test

The mechanical properties of the extruded alloys were evaluated by tensile test. Cylindrical specimen with the gauge length of 30 mm and diameter of 6 mm was machined from the as-extruded bar along ED. Tensile tests were carried out using a HT2008 machine under a constant strain rate of 5×10^{-4} s^{-1} at room temperature. Seven tensile specimens were tested for each alloy. The fracture surfaces were examined by a JSM-6700F SEM.

3 Results

XRD spectra (Fig.1) revealed that the major intermetallics in as-cast Mg-6Zn and Mg-6Zn-0.6Ce alloy was Mg_4Zn_7 phase. However, after extrusion the major compound was changed into $MgZn_2$ phase. In Mg-6Zn-1Ce and Mg-6Zn-2Ce alloys, the secondary phase was T phase under both as-cast and as-extruded condition. The diffraction peak of T phase in Mg-6Zn-2Ce alloy was more and stronger than that in Mg-6Zn-1Ce alloy, suggesting that Mg-6Zn-2Ce alloy contain more T phase.

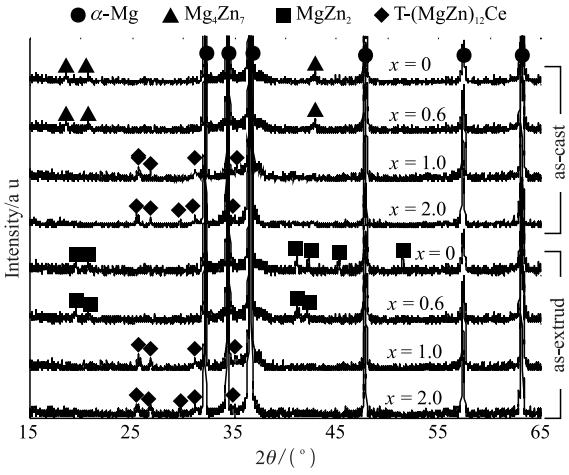

Fig.1 XRD spectra of Mg-6Zn-*x*Ce alloys

The microstructure of as-extruded alloys was composed of fine equiaxed grains due to the occurrence of complete dynamic recrystallization (Fig.2). The grain became slightly small with increasing content of Ce. The average grain sizes of Mg-6Zn-*x*Ce (*x*=0, 0.6, 1.0 and 2.0) alloys were 12.4, 11.7, 11.0 and 10.0 μm, respectively. In Mg-Zn-Ce alloys, the band microstructures distributed along ED was broken intermetallics particles, the volume fraction and density of which are increased with increasing Ce content. Relatively, there was no band microstructure in Mg-6Zn alloy.

SEM micrographs reveal the detailed morphology of broken intermetallic compound in Mg-Zn-Ce alloys (Fig.3). The high magnification SEM micrograph (the

insert in each figure) shows broken particles were irregular and concentrated locally. With increasing Ce content, the particle size increased slightly.

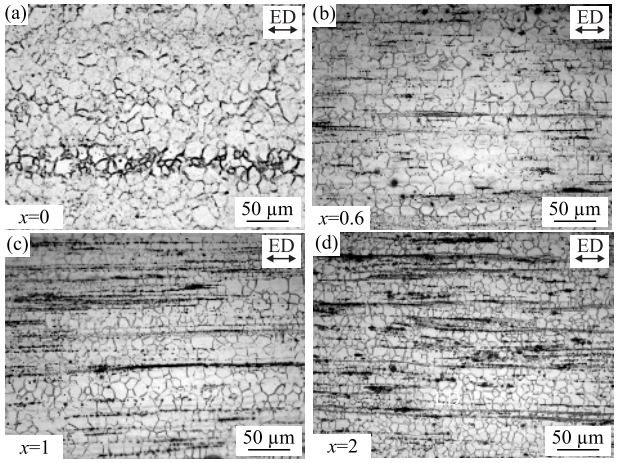

Fig.2 Optical micrographs of Mg-6Zn-*x*Ce alloys extruded at 300 ℃

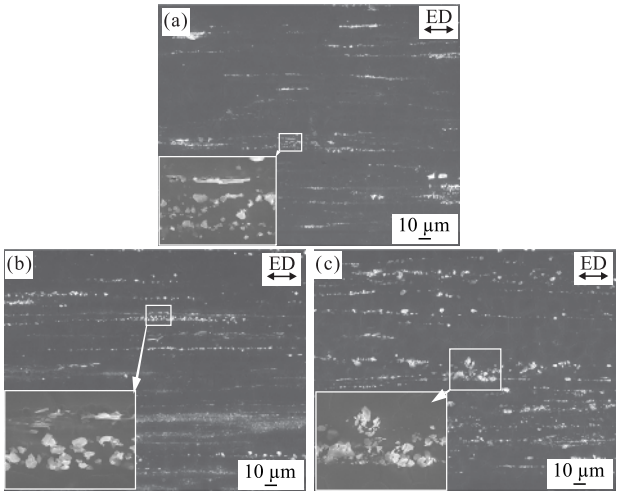

Fig.3 SEM images of Mg-Zn-Ce alloys: (a) Mg-6Zn-0.6Ce alloy; (b) Mg-6Zn-1Ce alloy; (c) Mg-6Zn-2Ce alloy

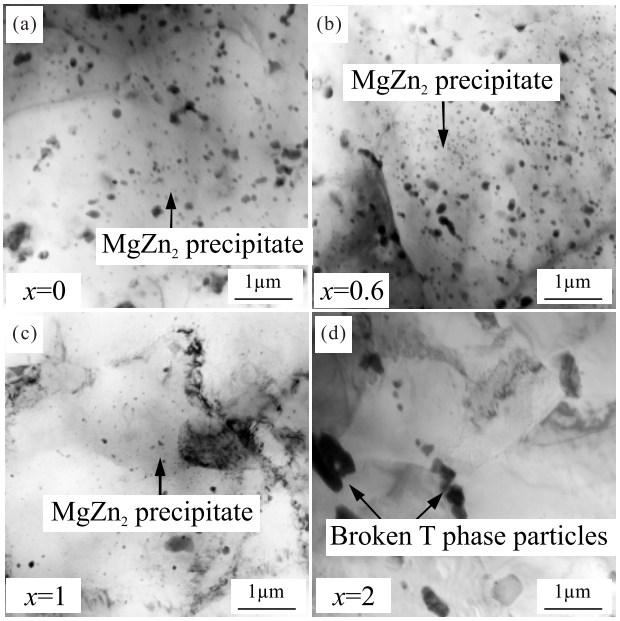

Fig.4 TEM images of as-extruded Mg-6Zn-*x*Ce alloys

TEM observations (Fig.4) found that dense precipitates with size smaller than 200 nm were distributed in the matrix of Mg-6Zn and Mg-6Zn-0.6Ce alloys, the average size of precipitate was about 60 nm. The density of precipitates of Mg-6Zn alloy was larger than that of Mg-6Zn-0.6Ce alloy. However, in Mg-6Zn-1Ce alloy the density of precipitates decreased evidently, and there were nearly free of precipitate in Mg-6Zn-2Ce alloy. According to XRD spectra it was reasonable to conclude that the precipitates were $MgZn_2$ phase, the large particles in Mg-6Zn-2Ce alloy (Fig.4(b)) were broken T phase.

Table 1 Tensile properties of as-extruded Mg-Zn-Ce alloys

Alloys	d /μm	σ_{YS} /MPa	σ_{UTS} /MPa	A /%
Mg-6Zn	12.4	202.6	289.5	14.3
Mg-6Zn-0.6Ce	11.7	226.3	304.2	12.8
Mg-6Zn-1Ce	11.0	223.5	302.7	10.1
Mg-6Zn-2Ce	10.0	212.8	298.8	9.5

The mechanical property test results (Table 1) revealed that a small amount of Ce had significant effect on tensile strength of Mg-6Zn alloy. With 0.6% Ce addition, the improvements of yield strength (YS) and ultimate tensile strength (UTS) were about 24 MPa and 15 MPa, respectively. However, with further increasing Ce content, the YS and UTS were decreased slightly. It is noted that the differences of YS and UTS between Mg-6Zn-0.6Ce and Mg-6Zn-1Ce was less than 5 MPa. Mg-6Zn alloy without Ce addition showed good ductility, and the elongation was decreased with increasing Ce content.

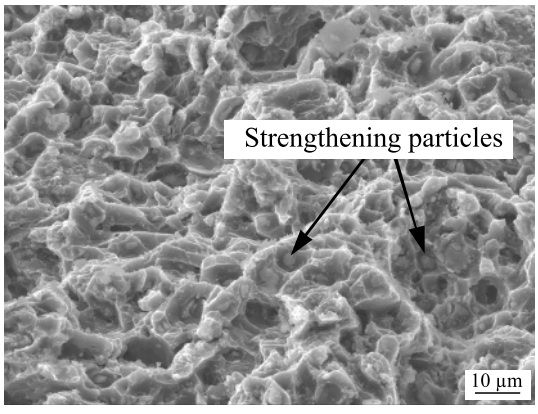

Fig.5 Fractural surface of Mg-6Zn-2Ce alloy

The fractures of Mg-6Zn-xCe alloys showed typical ductile morphology, a presentative fractural surface of Mg-6Zn-2Ce alloy is shown in Fig.5. The fracture was composed of uniform equiaxed dimples that was bounded by sharp lips or rims, each dimple

had a strengthening particle at the bottom.

4 Discussion

4.1 Microstructure

According to Mg-Zn phase diagram, the main intermetallics in Mg-6Zn alloy were Mg_7Zn_3 phase under equilibrium solidification process [13]. However, the solidification process can deviate the equilibrium solidification under the traditional casting condition owing to relatively rapid cooling rate, which leads to the formation of Mg_4Zn_7 phase by eutectic reaction at final stage of solidification. In this work, the primary intermetallics in as-cast Mg-6Zn and Mg-6Zn-0.6Ce alloys were Mg_4Zn_7 phase. The results were consistent with those reports [14, 15]. Moreover, it is noted that Mg_4Zn_7 phase is often observed during heat treatment[16,17].

With increasing Ce content Mg-Zn composition was decreased and volume fraction of T phase was increased. The phase transition was relative to the electronegativity value. The electronegativity difference between Ce and Zn was about 0.53, which was about 0.34 between Mg and Zn. Therefore, Zn atom was attracted easier by Ce atom, which resulted in the formation of T phase. A recent report found that T phase is a solid solution of $Mg_{12}Ce$ phase having a body-centered orthorhombic structure[18], and the solid solubility limit of Zn in $Mg_{12}Ce$ phase is 48.49 at% at 350℃[4]. With increasing Ce content, more and more Zn atoms were captured by T phase, which caused Mg-Zn compositions to decrease and disappear. Meanwhile, the number of Mg_2Zn precipitate was decreased dramatically due to rapid decrease of solid solubility of Zn atom in Mg matrix (Fig.4). In the alloy with 2% Ce content all Zn atoms almost were captured by T phase, hence the matrix was nearly free of precipitate.

The extrusion temperature approximated to eutectic temperature of Mg-Zn phase diagram and was hold for 1 h. Therefore, Mg_4Zn_7 phase was dissolved during extrusion process, and matrix was supersaturated solid solution. Afterward, Zn atoms dissociated from matrix as Mg-Zn precipitates, the procedure of which was spontaneous with the decrease of free energy. The major Mg-Zn precipitates in this study were $MgZn_2$ phase that was observed generally in wrought Mg-Zn alloys[22]. All $MgZn_2$ precipitates in extruded alloy were irregular near spherical particles, moreover, rod and block precipitates[2,19,20,21] were not detected. During heat treatment, the precipitates dissolved out thought G.P. zone and grow along preferential orientation. However, during extrusion process, precipitates nucleated prior at distortion region of crystal lattice, and it was hard to grow along preferential orientation direction. On the other hand, precipitate was subject to shear stress from different directions. Therefore, precipitates were irregular and hard to grow up to rods and plates.

We previously studied the microstructure of rapidly solidified ZK60 alloy and found that Zn atoms dissolve out leeching on to dislocation to form Cottrell atmosphere[23]. The required phase boundary energy of a precipitate nucleated from Cottrell atmosphere was smaller than that from intact grain interior, and the boundary of cross-slip was preferential nucleation site. Therefore, the nucleation period of Mg-Zn precipitate in hot extruded condition was shorter than aging treatment. Moreover, Ce stimulates the Mg-Zn precipitate nucleation has been clarified[24]. Ce dissociated from Mg solid solution, thereby providing suitable (heterogeneous) nucleation sites for the aggregation of Zn atoms, leading to the formation of the stable precipitate nuclei in a very short period after extrusion. Therefore, Mg-6Zn and Mg-6Zn-0.6Ce alloys contain high density of precipitates, and the precipitates in Mg-6Zn-0.6Ce was denser than Mg-6Zn alloy.

The DRX grain size was bound up with density and distribution of strengthening particles. A large number of dislocations were generated during extrusion. The strengthening particles can prevent the movement of dislocation, resulting in dislocation to be pile up around the particle, which improve nucleation rate of DRX grain. In addition, strengthening particle can pin grain boundary to retain the movement of grain boundary, thus the grain growth was restricted. Generally, the more alloying element be added, the larger volume fraction and denser of secondary phase particle were, and smaller DRX grains were. In present study with increasing Ce content the volume fraction and density of T phase particle was increased along extrusion direction (Fig.3). Meanwhile, TEM micrographs revealed dense precipitates distributed on the matrix in Mg-6Zn alloy, and the volume fraction of precipitate was decreased with increasing Ce content, which is because T phase consumes a large number of Zn atoms. On the whole, the increase of the total volume fraction of strengthening particle was small. Therefore, the difference of grain size between among the 300 ℃ extruded Mg-6Zn and Mg-6Zn-2Ce alloys was only 2 μm.

4.2 Mechanical properties

Mg-6Zn-*x*Ce alloys had approximate grain size; therefore, the difference of yield strength is ascribed to the comprehensive contributions of particle strengthening of broken T phase, precipitation strengthening of $MgZn_2$ and solid solute strengthening of Zn atom. According to the analytic results of TEM and SEM, with increasing Ce content particle strengthening effect was enhanced, precipitation strengthening and solid solute strengthening were weakened. Therefore, the variation of strength was nonlinear. Comparing with the strength of Mg-6Zn and Mg-6Zn-2Ce alloys it is implied that the contribution of particle strengthening of T phase almost equaled to total contribution of precipitation strengthening and solid solution strengthening. Hence, the strength depended on the comprehensive contribution of above strengthening factors. It is noted that the yield strength was improved significantly with 0.6% Ce addition for Mg-6Zn alloy, suggesting Ce element had good strengthening effect for Mg-Zn alloys, which could be ascribed to the dense $MgZn_2$ precipitates and broken T phase particles. In Mg-6Zn-1Ce alloy, the density of $MgZn_2$ precipitate was decreased rapidly but the quantity of broken particle was increased and the solid solution strengthening was conserved. Therefore, its strength approximates to that of Mg-6Zn-0.6Ce alloy.

Previous reports found that a trace amount of Ce could significantly improve the ductility of Mg alloys[8]. However, this work showed the elongation of Mg-6Zn-0.6Ce was less than that of Mg-6Zn alloy, and the elongation was decreased with increasing Ce addition, which was ascribed to fractural mechanism. It is established that a trace amount of Ce addition favors the formation of DRX grains with their basal planes oriented at 40°-50° to extrusion axis, which results in significant increase of elongation in Mg alloy. However, the prerequisite is that almost all alloying elements are dissolved into matrix. Hence, previous theory can apply to the alloys containing a small amount of alloying elements, for example Mg-0.2Ce[8] and Mg-1.5Zn-0.2Ce[11] alloys. The alloys in our study contain more alloying elements and a large number of secondary phase particles. Hence, the fracture was determined by size and density of strengthening particles. Under tensile stress dislocation pile-up occurred primarily at the interface of broken secondary phase particles and matrix. Then microvoids formed at the interface of particle and matrix. The microvoids experienced the growth, and finally the interlinkage of microvoids resulted in the failure of the material. The strengthening particles in Mg-6Zn alloy were smaller than Mg-Zn-Ce alloy; the stress concentration effect accordingly was weaker. Therefore, Mg-6Zn alloy showed better ductility than Mg-Zn-Ce alloy.

5 Conclusions

a) The major intermetallic composition in as-cast Mg-6Zn and Mg-6Zn-0.6Ce alloys was Mg_4Zn_7 phase, during extrusion Mg_4Zn_7 phase was dissolved into matrix and then precipitated as $MgZn_2$. In as-cast and as-extruded Mg-6Zn-1Ce and Mg-6Zn-2Ce alloys the major intermetallic composition was T phase.

b) The microstructure of as-extruded alloy was refined due to complete dynamic recrystallization, the average grain size decreased with increasing Ce content, the grain sizes of Mg-6Zn-*x*Ce (*x*=0, 0.6, 1.0, 2.0) alloys were 12.1, 11.7, 11.0, 10.0 μm, respectively. The broken T phase particles were distributed linearly along extrusion direction. The average size of $MgZn_2$ precipitate was about 60 nm, with increasing Ce content the density of precipitate was decrease. There was almost free of $MgZn_2$ precipitate in Mg-6Zn-2Ce alloy.

c) Mg-6Zn-0.6Ce alloy exhibited a good yield strength of 226.3 MPa that was about 24 MPa higher than Mg-6Zn alloy. The strengthening effect of T phase was enhanced by adding more Ce content, however, the effects of precipitation strengthening and solid solute strengthening were weakened, which resulted in the slight decrease of strength. The elongation was decreased with increasing Ce content.

References

[1] Arruebarrena G, Hurtado I, VÄINÖLÄ J, *et al*. Development of Investment-Casting Process of Mg-Alloys for Aerospace Applications[J]. *Adv. Eng. Mater.*, 2007, 9(9): 751-756

[2] Buha J. Reduced Temperature (22-100 ℃) Ageing of an Mg-Zn Alloy[J]. *Mater. Sci. Eng. A*, 2008, 492(1-2): 11–19

[3] Buha J. The Effect of Ba on the Microstructure and Age Hardening of an Mg-Zn Alloy[J]. *Mater. Sci. Eng. A*, 2008, 491(1-2): 70-79

[4] Kevorkov D, Pekguleryuz M. Experimental Study of the Ce-Mg-Zn Phase Diagram at 350 °C via Diffusion Couple Techniques[J]. *J. Alloys and Comp.*, 2009, 478(1-2): 427-436

[5] Yang W P, Guo X F. A High Strength Mg-6Zn-1Y-1Ce Alloy Prepared by Hot Extrusion[J]. *J. Wuhan Univ. of Tech*., 2013, 28(2): 389-395

[6] Yang W P, Guo X F. High Strength Magnesium Alloy with α-Mg and W-phase Processed by Hot Extrusion[J]. *Tran. Nonferr. Metals Soc. China*, 2011, 21(11): 2 358-2 364

[7] Yi D, Wang B, Fang X, *et al*. Effect of Rare-Earth Elements Y and Ce on the Microstructure and Mechanical Properties of ZK60 Alloy[J]. *Mater. Sci. Forum*, 2005, 488-489: 103-106

[8] Mishra R K, Gupta A K, Rao P R, *et al*. Influence of Cerium on the Texture and Ductility of Magnesium Extrusions[J]. *Scripta Mater.*, 2008, 59(5): 562-565

[9] Luo A A, Mishra R K, Sachdev A K. High-Ductility Magnesium-Zinc-Cerium Extrusion Alloys[J]. *Scripta Mater.*, 2011, 64(5): 410-413

[10] Cai J, Ma G C, Liu Z, *et al*. Influence of Rapid Solidification on the Mechanical Properties of Mg-Zn-Ce-Ag Magnesium Alloy[J]. *Mater. Sci. Eng. A*, 2007, 456(1-2): 364-367

[11] Chino Y, Sassa K, Mabuchi M. Texture and Stretch Formability of Mg-1.5 mass %Zn-0.2 mass % Ce Alloy Rolled at Different Rolling Temperatures[J]. *Mater. Tran*., 2008, 49(12): 2 916-2 918

[12] Zhou T, Xia H, Chen Z H. Effect of Ce on Microstructures and Mechanical Properties of Rapidly Solidified Mg-Zn Alloy[J]. *Mater. Sci. Tech.*, 2011, 27(7): 1 198-1 205

[13] Okamoto H. Comment on Mg-Zn (Magnesium-Zinc)[J]. *J. Phase Equilibria*, 1994, 15(1): 129-130

[14] Alizadeh R, Mahumudi R, Langdon T. Creep Mechanisms in an Mg-4Zn Alloy in the As-cast and Aged Conditions[J]. *Mater. Sci. Eng. A*, 2013, 564: 423-430

[15] Gao X, Nie J F. Characterization of Strengthening Precipitate Phases in a Mg-Zn Alloy[J]. *Scripta Mater*., 2007, 56(8): 645-648

[16] Wei L Y, Dunlop G L, Westengen H. The Intergranular Microstructure of Cast Mg-Zn and Mg-Zn-Rare Earth Alloys[J]. *Metall. Mater. Tran. A*, 1995, 26(8): 1 947-1 955

[17] Wei L Y, Dunlop G L, Westengen H. Solidification Behaviour and Phase Constituents of Cast Mg-Zn-Misch Metal Alloys[J]. *J. Mater. Sci*., 1997, 32(12): 3 335-3 340

[18] Yang W P, Guo X F, Lu Z X. Crystal Structure of the Ternary Mg-Zn-Ce Phase in Rapidly Solidified Mg-6Zn-1Y-1Ce Alloy[J]. *J. Alloys Comp*., 2012, 521: 1-3

[19] Buha J. Grain Refinement and Improved Age Hardening of Mg-Zn Alloy by a Trace Amount of V[J]. *Acta Mater.*, 2008, 56(14): 3 533-3 542

[20] Rosalie J M, Somekawa H, Singh A, *et al*. Structural Relationships among $MgZn_2$ and Mg_4Zn_7 Phases and Transition Structures in Mg-Zn-Y Alloys[J]. *Philos. Mag.*, 2010, 90(24): 3 355-3 374

[21] Singh A, Tsai A P. Structural Characteristics of β_1' Precipitates in Mg-Zn-Based Alloys[J]. *Scripta Mater.*, 2007, 57(10): 941-944

[22] He S M, Peng L M, Zeng X Q, *et al*. Comparison of the Microstructure and Mechanical Properties of a ZK60 Alloy with and without 1.3 wt% Gadolinium Addition[J]. *Mater. Sci. Eng. A*, 2006, 433(1-2): 175-181

[23] Yang W P, Guo X F, Yang K J. Low Temperature Quasi-Superplasticity of ZK60 Alloy Prepared by Reciprocating Extrusion[J]. *Tran. Nonferr. Metals Soc. China*, 2012, 22(2): 255-261

[24] Chino Y, Huang X, Suzuki K, *et al*. Influence of Zn Concentration on Stretch Formability at Room Temperature of Mg-Zn-Ce Alloy[J]. *Mater. Sci. Eng. A*, 2010, 528(2): 566-572